Combining Biometrics Derived from Different Classes of Nonlinear Analyses of Fronto-Normal Gait Signals

T. K. M. Lee
School of IT, Monash University
Sunway Campus, Malaysia
School of EEE, Singapore Polytechnic,
Singapore
tlee@sp.edu.sg

S. Sanei
Faculty of Eng. & Physical Sciences,
University of Surrey, Surrey, UK
s.sanei@surrey.ac.uk

M. Belkhatir
Faculty of Computer Science,
University of Lyon & CNRS, France
mohammed.belkhatir@univ-lyon1.fr

Abstract– With the advent of low cost high powered computing, cameras need not just be used to record multimedia data. Cameras become sensors as we process waveforms of gait signals from the video content of humans walking towards these cameras. This sensory data allows cameras to be incorporated into networks that monitor humans and their movements. This work introduces a novel analysis of gait for human recognition which uses and can be used for surveillance. Current approaches in human gait analyses employ linear signal decomposition techniques to obtain features such as frequency and phase. In contrast, we establish the nonlinear nature of fronto-normal (FN) gait. This motivates for the use of nonlinear analyses on FN gait as a biometric and opens up new avenues for research in gait recognition. Using these nonlinear analyses to derive features, we show that by themselves they may not provide sufficient discriminating ability. But by a novel combination of two different nonlinear measures, one exploiting chaosity and another representing regularity, this can be used to identify a person using gait. We apply this in a multi-biometric experiment to demonstrate its effectiveness.

Keywords-gait, nonlinear; chaos; Hilbert Huang Transform; EMD

I. Introduction

Due to the current security climate, the presence of multimedia devices such as low cost webcams and security cameras are well nigh ubiquitous, whether in points of access or traffic. But these cameras may not just be used to capture image and video data as the information can be used to *sense* the environment and be processed to produce sensory data. This is important as cameras are being deployed in networks to so that multiple views and interpretations of a scene can provide a more robust analysis of the same. For example, the static images that come from a camera can be used for face recognition which in effect, senses the presence of a particular person. Considering the video component of the data, it is more than just a stream of static images. They incorporate a temporal dimension which can be used to derive time-based features such as frequency of the movement of the limbs while walking which comprises the gait of a person. Effectively, this makes the camera a gait sensor, which does not require attachment to a person. Gait or the manner of walking of a person, is a biological feature - its fundamental properties have been established in medical studies.

Recently, gait has been considered as a biometric which is a registered biological trait, used in human identification. Gait includes static features such as height, stride length and silhouette bounding box lengths. Some dynamic features of gait are frequency domain parameters like frequency and phase of a walk. As a biometric, gait has desirable properties, primarily because it is hard to disguise, as in normal circumstances gait movement is involuntary. Furthermore, it can be used at long distances, and it is non-intrusive and non-invasive. In the literature, the main gait recognition approaches analyze walking which proceeds in a plane parallel to a camera, the so-called fronto-parallel (FP) view. This gives the largest variation in a silhouette from which time series data is obtained for analysis. From a far distance, this is advantageous. However, being able to obtain these silhouette images from a far distance require a clear, uncluttered field of view.

As a contrast, a very common scenario is when people queue up to access a facility. In a corridor like structure, we assume that a subject is approaching a camera. In such situations gait can be used as a supporting biometric because as the subject draws nearer, other biometrics such as face or iris can be used for robust recognition. Motion in this plane which is perpendicular to the FP view, is the fronto-normal view (FN) which is considered as a special case of FP gait. Depending on the type of analysis need, in a FP walk, at least two cycles or four steps are needed. For more robust estimation of the period of walking, about 8 m is recommended [1]. To capture this movement, the camera distance required is about 9 m [2]. This is because current video cameras typically have a focal length and sensor size of 8 mm and 1/2" respectively. Practically, having such a wide uncluttered space is difficult, since whenever we want to measure a person's gait, many people and objects will be present.

In a FN view, we can still use the 8 m. But this time, we cover twelve steps and we only need a corridor-like structure, the width being about that of a human body. Therefore, a considerable amount of space is saved as shown in Figure 1 in this case, by 2/9. Besides the considerable advantages in savings of physical space and better viewpoint, Lee et al. have put forth the advantages of the monocular FN non-silhouette approach as [3]:

i) Smaller physical space is needed.
ii) Multiple subjects can be tracked.
iii) Other biometrics can be easily combined.
iv) Wide variety of time analysis including non-periodic motion analysis can be used.
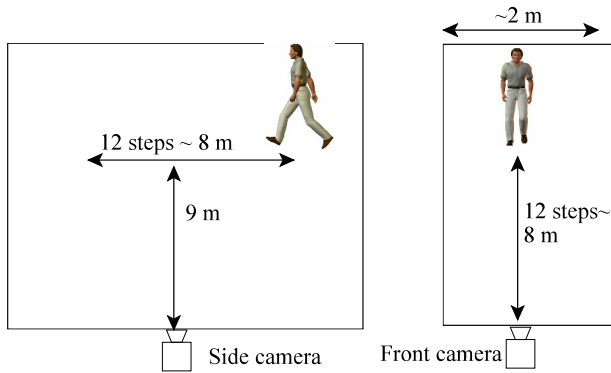

Figure 1. FP vs FN - physical dimensions for video capture

This approach has its own unique challenges when fast and reliable recognition is necessary. There are some recent surveys on gait recognition such as that done by Lee et al. [4] Most gait recognition approaches use a combination of static and dynamic gait features. Dynamic features are usually linear, like frequency of walking. Using time series parametric models for gait recognition is fairly recent, for example by Veeraghavan et al. in [5]. Lee et al. showed that chaotic measures may be used to help identify people by their gait [6]. In another paper, they show that FN gait data is mainly stationary [7]. Recently, they have also combined nonlinear measures to provide a more robust gait recognition process [8]. With respect to that publication [8] this paper renders a more complete treatment of the approach.

Many analyses of gait data assume the property of linearity without testing for it. Linearity refers to how the data may be generated by the scaled linear sums of input signals. Elaborating on this concept leads ultimately to convolution, a linear operation much used in signal processing. In the main, dynamic features of gait have been obtained by linearly decomposing gait signals via the Fourier transform, which is extensively used and has a good mathematical foundation. However, most analyses do not check that the signal is linear and stationary in nature. The gait signal is assumed to be statistically stationary. However, most biological signals are not so well specified, many studies showing that they are nonlinear and nonstationary especially in the FN. Based on biological evidence and using our FN gait dataset, Lee et al. have shown that dynamic gait data is in fact nonlinear and thus should be analyzed using nonlinear methods [9]. Applying Fourier-based decomposition to nonlinear and nonstationary signals produce mathematically correct functions, but these may not have any physical meaning at all. These signal constituents serve only to accommodate the lack of linearity and stationarity. This limits the use of such analyses in processing the signal. There are many methods to decompose

data so it can be expressed in terms of components that combine in a linear way. For each of them, there are much more ways to do so nonlinearly as described by Tong, which gives rise to a rich source of features to be used in pattern recognition [10]. In this paper, we look at two of the more prominent methods of nonlinear analyses to derive features for recognition. We combine these features to increase their robustness for this task. The novelty of our approach lies in the use *and* fusion of nonlinear features for the recognition task. We demonstrate the efficacy of our approach in an experiment. In Section II, we look at the current state of temporal gait analysis. Section III covers our setup and preliminary results, Section IV describes the theory behind using Chaos Theory and the Hilbert Huang Transform (HHT) for analyzing FN gait. Section V shows some results with preliminary analysis and we conclude with Section VI.

A. Overview of temporal Gait Analysis

Psychophysical experiments using Moving Light Displays (MLDs) attached to humans have shown the possibility of using gait for identification purposes. Some time ago, Johansson showed how the patterns traced by MLDs can be perceived as that of people walking [11]. Cutting and Kozlowski showed that identification was possible from MLDs [12]. Recently, Troje has shown that the task of recognizing gender from MLDs has a lower error rate using a frontal view [13].

Gait as a biometric can be used at long distances, is non-intrusive, non-invasive, and is hard to disguise. From the medical literature (such as [1]), gait information is obtained via sensors directly attached to the body. With image processing, gait is derived from the 2D image projected on a camera sensor. In this section, we provide a brief overview of human recognition using gait with time-based features. Gait includes static features such as height, stride length and silhouette bounding box lengths. Some dynamic features of gait are frequency domain parameters like frequency and phase of a walk, which also includes the bounding box of the walking silhouette. In the literature, the area of gait analysis and recognition has involved medical analyses looking for exact movement of body parts to detect pathological conditions. Rather than standard approaches which use body silhouettes as ably described by Nixon et al., we consider the motion of individual body parts like hands and feet [14]. These produce biologically based spatio-temporal signal features which can be used as a biometric.

Much of the current gait analyses use silhouettes in the FP view because of the large changes in shape and most of these analyses assume that the signal derived from gait are linear and stationary for the sake of simplicity. Linearity refers to how the data may be described by the scaled, linear sums of input signals. In what follows, we consider a signal, which can be considered a set of time series data $\{x(t_i)\}$ for $i = 1..N$ sample points. In general, we say s is in a linear signal space if :

$$s(t) = \sum_{k=-\infty}^{\infty} h(k)\, x(t-k) \qquad (1)$$

where $h(k)$ are constants and the inputs $x(t)$ may be generated

by functions $f(t)$. That is, the data may be generated by the scaled, linear sums of input signals. The equation is cast as a convolution which is a common linear operation.

Stationarity entails having the statistical properties of the signal up to the second order to be constant in time. That is, $k_p = E[x^P(t)]$ where k_p is a constant, $E[\cdot]$ is the statistical expectation operator and p is the order. Usually the first order statistic is the mean, and the second order statistic the variance but sometimes the autocovariance or autocorrelation function of the signal. These measures have been used to analyze gait by decomposing the signal into its constituents. A common linear example, which has been well developed is the Fourier expansion, where the $f(t)$'s are sinusoidal functions. Current approaches have used this successfully because the FP view of gait is particularly amenable to linear analysis in contrast to the FN gait, as shown by Lee et al. [8] This motivates a search for nonlinearity and nonstationarity in descriptions of data which can be used as biometrics. In this work, they show that FN gait can be characterised by nonlinear measures. A variety of time series analyses from the fields of econometrics and physics may be employed to further characterize the gait. In contrast, FP gait yields mainly periodic measures.

Ibrahim et al. have used Empirical Mode Decompostion (EMD) (described in Section III.C) to detect the *type* of gait of a subject using a 3D accelerometer using the energy of its Intrinsic Mode Functions (IMF) [15]. From the same research group, Wang et al. have looked into various features based on IMFs and the features associated with Hilbert spectra for *clinical* gait analysis [16].

Kuchi et al. have used EMD for gait recognition. But we note that they use motion capture equipment, where the coordinates of markers attached to the body are computed in-camera at data rates of 120 samples/s [17]. Thus, the cameras are not designed to give video information. They analyze the signal for one walk cycle and for one marker, giving encouraging results. However, they do not analyze their data to provide justification for using nonlinear, nonstationary analyses. We also feel that extending the results to ordinary video cameras that can be used in security checkpoints is difficult.

II. EXPERIMENTAL SETUP

We used a commercial video camera with a capture rate of 25 frames/s at 720 by 480 resolution. In gait recognition from video, we use feature points that have more motion in the camera plane. This would be the hands, feet, and knees for a FP walk. For a FN walk this is also true, although the motions are smaller in magnitude. For the two kinds of walk, we show the coloured marker set up in Figure 2. The marker designations are: *lh/rh* - left/right hand: *lf/rf* - left/right foot and *lk/rk* - left/right knee. Two additional discs of the same colour are attached at the waist and face level which are used for distance normalization. They are: *tm/bm*, the top/bottom markers. The markers are tracked using the CAMSHIFT algorithm [18]. We take video clips of twelve subjects and a further three for testing. Since in a FN walk, there is the looming effect caused by the subject approaching the camera. This causes the movements to grow larger and show a definite

trend in the data as will be seen in Figures 3 and 4. The data trend is immediately removed and normalized in the following way:

i) Use the coordinates of the *bm* marker as the origin of the markers.
ii) The length between the *tm/bm* markers are used to divide the distance between the *bm* marker and the other marker coordinates.

Thus every subject will have 12 time series associated with the *x* and *y* movements of the 6 markers attached to the body, for a FN walk. We have 12 subjects giving a total of 144 time series. In a FP walk, we have only 6 time series from 3 markers and 2 sequences, giving 12 time series. This is because analysis using FP data are well documented in the literature.

Of the gait datasets currently available, most are of the FP view taken at low resolution. Features for recognition include frequencies of motion from Fourier-based decomposition of the motion signal. As described by Lee et al. [19] these gait datasets are not suited for our use and there are few substantial video sequences of FN gait available. Thus we create and explore the use of a dataset that focuses on and exploits the advantages of the FN view. The experience gained in using this smaller dataset will serve to prepare for larger scale work. We have FP gait sequences which are used for confirmatory tests of linearity only.
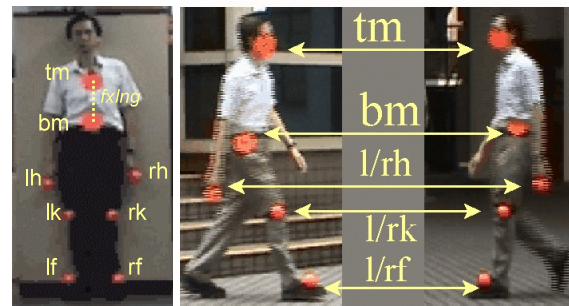

Figure 2. Marker positions: Left - FN view Right - FP view

III. THEORETICAL CONSIDERATIONS OF NONLINEAR SIGNAL ANALYSIS AND DATA ANALYSIS PROCEDURE

This section looks at the theory used to analyze the linearity of gait signals. The plot of the autocorrelation function (*ac.f*) gives a quick visual indicator of the nature of the signal. Of the several analytical methods available, there are those based on frequency domain approaches like that of the bispectrum or higher order moments which do not need parameters. In the time domain, Autoregressive (AR) and Moving Average (MA) models are popular. These methods model the human walk using a set of computed parameters.

A. Testing for nonlinearity using nonparametric methods

The nonparametric method of surrogate data introduced by Theiler et al. [20] uses a more general form of statistical hypothesis testing where we postulate the null hypothesis of

linearity. Then *simulated* data are generated from the processes which are known to have linear and stationary properties. A discriminating statistic is computed on the simulated data and a *critical* value determined, based on various levels of significance for which the hypothesis holds.

Using the *experimental* data now, the discriminating statistic is again computed and compared with the critical values which now act as threshold values. We seek to reject the null hypothesis so that the alternative is true - i.e., the presence of nonlinearity. Surrogate data is one way to obtain *simulated* data conforming to the null hypothesis. The steps are:

i.   A Fourier transform (FT) is applied to the data.
ii. In the transformed data, the phase is randomized.
iii. The data set is converted back to the time domain.

The surrogate data has linear properties and maintains the stationary properties of the original data, like the variance and autocorrelation. Various modifications on the basic algorithm refine on how well the stationary properties are kept. Thus the surrogate data are Gaussian, linear and stationary. Many sets of surrogate data can be generated by changing the random seed. Using surrogate data requires a suitable discriminating statistic to be determined from *both* experimental and surrogate data and a comparison made. Schreiber and Schmitz showed that a statistic based on nonlinear predictor errors (NPE) gives good results for detecting nonlinearity as compared to several others [21]. The null hypothesis of linearity postulates that the NPE computed from the original data lies within normal variation limits with the NPE obtained from sets of surrogate data [22]. Nonlinearity points the way to novel methods of analysis such as that used in chaos theory.

For the sake of completeness, we include a brief discussion about the use of prediction as a test of linearity - a fuller account may be found in [23]. Assuming a signal with a deterministic structure, its *predicted* values in the short term may be expressed as a *linear* weighted sum of its previous values in the time domain as described in (1). Of course, we will use values already in the time series to compute the prediction error. If the previous values are shuffled around as in the case of surrogate data, there will be a large variation in the short term predicted values of the surrogate data. However if we use a suitable nonlinear prediction method which does not depend on linear computations, the predicted values should not vary so much in the surrogate data. This approach uses nonlinear prediction in phase space as explained in Section III.B.

Of the many ways of characterizing nonlinear behaviour, we select the most widely used from two major categories. The first consists of examining its overall behaviour using phase space approaches. A widely used method invokes deterministic chaos theory. Another set of approaches is similar to linear analysis, but this time the signal is split into constituent nonlinear functions. For the sake of completeness, we describe an earlier work of ours using a measure of chaos, namely the Largest Lyapunov Exponent, or λ_1 to characterize gait [8].

B. Measuring Chaos with Lyapunov Exponents

To test for nonlinear chaotic behaviour, a *scalar* time series is subjected to dynamical analysis which assumes that the time series data x is generated by a vector valued process. The actual state vectors describing this process may never be known. But we can create a set of *phase space* vectors which are topographically equivalent, and can be considered to be a reconstruction of them. Takens' "method of delays" is an established method for doing this [24]. He also shows that if the dimension of the phase space vectors m is larger than the dimension of the *chaotic* attractor D, we can say that the phase vectors *embed* the state vectors and $m > 2D + 1$. Thus the reconstructed trajectory of X is made up of several phase space vectors as follows:

$$X = [X_1\ X_2 \ldots X_m]^T$$

where X_i is the state of the system at sample i. Each row of X is a phase-space vector with a length of the embedding dimension m. That is, for each X_i,

$$X_i = [\ x_i\ x_{i+\tau} \ldots\ x_{i+(m-1)\tau}\ ]$$

where τ is the time lag for a time series $x = \{x_1, x_2, \ldots, x_N\}$ with N points. So X is an M by m matrix, and we have M the number of phase space vectors being $N - (m - 1)\tau$. The set of phase vectors describes a path or a trajectory in m dimensional space, and analyzing its behaviour gives a measure of chaos.

For parameter τ, the standard method is to take the time when the autocorrelation plot first goes to zero. But in Figure 7 we see that it never reaches zero until the end of the walk, so we use the time delayed mutual information measure as proposed by Fraser and Swinney [25]. For parameter m, we use the method of false nearest neighbours (FNN) proposed by Kennel et al. in [26].

In characterizing chaotic behaviour, the largest Lyapunov exponent λ_1 is the most useful and commonly used measure. If the system equations generating the data are known, it is quite straightforward to calculate it. λ_1 describes how quickly trajectories approach or come together, given different initial conditions. This comes directly from a definition of chaos. Then λ_1 is the mean exponential rate of divergence of two initially close trajectories from an initial time t_0 to t_i. The divergence d_j between the jth set of points on the two trajectories is the Euclidean distance between them.

$$\lambda_1 = \frac{1}{t_i - t_0} \sum_{k=1}^{i} \log_2 \frac{d(t_k)}{d(t_{k-1})} \qquad (2)$$

One of the more recent methods to calculate λ_1 was formulated by Rosenstein [27] and independently, by Kantz [28]. This method is suitable for small and noisy data sets. Assume a fixed sampling time period Δt and that at t_i the sample number is i so that $t_i - t_0 = i\Delta t$. We substitute the subscripted time t_i by its index i. Taking logarithms on both sides of (2), we have:

$$\log_2 d_j(i) = \lambda_1 i\Delta t + \log_2 d_j(0)$$

The initial separation $\log_2 d_j(0)$ is constant, so we have a group of $j = 1$ to M (phase space vectors) approximately parallel lines for the sample number i. The main feature of this method is that we average the $\log_2 d_j(i)$ values for all j pairs of sample points at each sample j. Then

$$\langle \log_2 d_j(i)\rangle / \Delta t = \lambda_1 i + \langle \log_2 d_j(0)\rangle / \Delta t \qquad (3)$$

where $<\cdot>$ is the average operator. We average further by fitting a line using Least Squares to the "average line" of (3) after which, λ_1 is the slope of the fitted lines. This will be shown in Section V.

C. The Hilbert Huang Transform

Recently, the EMD technique has been used for signal analysis and decomposition. Huang et al. pioneered its use in ocean wave studies [29]. It was motivated by the need to study nonlinearity and nonstationarity by obtaining the instantaneous frequency and amplitude of a signal as defined in (5). These allow us to see where the signal is changing, but the difficulty lies in the *scale* of the change, for example intermittent background noise in a larger say, audio signal. Traditional time-frequency signal processing methods like the Fourier Transform wavelet analysis do not provide a sharp distinction between the various harmonic components of the signal [30].

The HHT attempts to overcome this problem in a two-step process. Firstly, EMD decomposes a signal into a set of constituent functions, which are the IMFs at suitable scales of the signal. These functions are then subject to the Hilbert Transform which gives amplitude and phase information over the duration of the signal from which we obtain the instantaneous frequency and amplitude.

1) IMFs and the sifting process

Assuming the signal is oscillatory, IMFs have two special properties - firstly, the number of extrema and zero crossings must be equal or differ by one. Secondly, the envelope of a signal touching the local maxima and the envelope touching the local minima of the IMF has a local mean value of zero. The signal $x(t)$ is decomposed into its IMFs through the process of sifting. Rather than fitting a predefined mathematical procedure, this works with the signal data directly. For the first function IMF_1:

   i. locate all the extrema of $x(t)$
   ii. generate the envelope signals touching the maxima and minima $e_{max}(t)$ and $e_{min}(t)$ respectively
   iii. obtain the mean signal $m(t) = (e_{max}(t) + e_{min}(t))/2$
   iv. from the original and mean signal, obtain the residual signal $r(t) = x(t) - m(t)$
   v. iterate steps i to iv by substituting $r(t)$ into $x(t)$ until a given criterion is met. The residual signal is IMF_1.

The next function IMF_2 is derived by using $x(t) - m(t)$ in place of $x(t)$ above. The whole process stops when a monotonic IMF is obtained. IMFs may or not have constant amplitude and frequency and can be used to reconstitute the original signal, or for further processing. In our case, the Hilbert Transform is applied to each IMF obtain the instantaneous frequency.

2) The Hilbert Transform

The Hilbert Transform computes the conjugate function $y(t)$ of any real valued function $x(t)$. By doing so, an analytic function $z(t) = x(t) + iy(t)$ is defined. In polar form:

$$z(t) = a(t)e^{i\theta(t)} \text{ where } a(t) = \sqrt{x(t)^2 + y(t)^2}$$
$$\text{with } \theta(t) = \arctan\frac{y(t)}{x(t)} \text{ so that } \omega(t) = \frac{d\theta(t)}{dt} \qquad (4)$$

where $\omega(t)$ and $a(t)$ are the instantaneous frequency and amplitude, respectively at time t. From this, other measures like the mean instantaneous frequency (*MIF*) and the weighted mean instantaneous frequency (*WMIF*) can be derived for *each* IMF of the original signal. Then using quantities defined in (4)

$$MIF = \frac{1}{N}\sum_{t=1}^{N}\omega(t) \qquad WMIF = \frac{1}{N}\sum_{t=1}^{N}a(t)\omega(t) \qquad (5)$$

for N samples, for a given IMF.

3) Analysis procedure

Since there is such a wide range of data, we perform a simple data reduction operation for ease of analysis. We use the simple average of the *WIMF*s of all the markers of a subject, looking for those which remain relatively constant for separate gait sessions. This is done to use as much idiosyncratic information as possible.

IV. RESULTS FROM PRIOR EXPERIMENTS

This section covers the waveforms obtained from tracking body parts and the results required for nonlinear analyses of signals from previous publications and have been reproduced here for the sake of completeness. The results concern the tests for linearity or the lack of it and the derivation of parameters required for proper embedding of data as explained in Section III.B.

As described earlier, the subjects in our dataset are designated by symbols such as *s01*, *s02*, *s04* and so on. Those having the suffix 'a' are the second video sequence of the subject, as *s02a* is the second video from *s02*. The unnormalized and normalized plots for a FP walk are shown in Figures 3 and 5 respectively. In this figure, the x-axis motion would seem to swamp out that of the y-axis. This can be visualized for example, that the horizontal left to right motion of an arm swing is larger than that of the vertical motion.
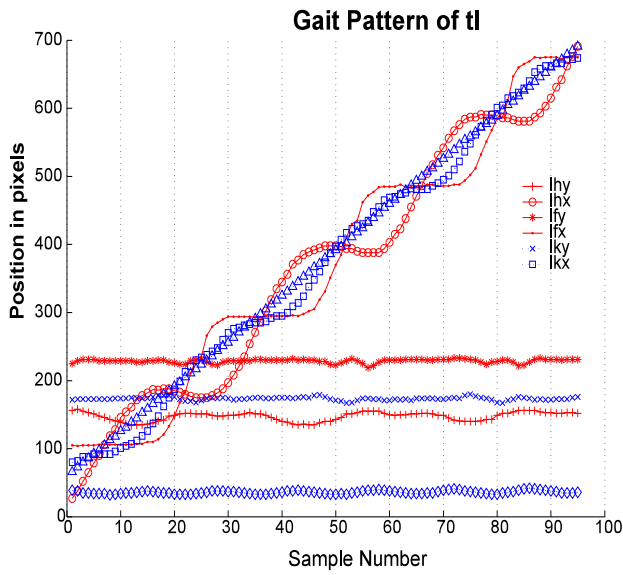
Gait Pattern of tl

Figure 3. Unnormalized plot of a FP walk

In Figure 3 we note the motion of the body parts, in particular the x-axis coordinates which show an increase with a linear trend, reflecting the steady walking speed of the subject. By normalizing, we obtain the periodic waveform shown in Figure 5.

As a comparison, the corresponding plots for the FN walk are shown in Figures 4 and 6. In Figure 4 the coordinates increase with a nonlinear trend, a consequence of the physics of a thin lens. Here the dimensions of an object in the lens' focal plane varies inversely with the object distance from the lens [31]. However, the normalized plot in Figure 6 gives a semblance of a periodic waveform.
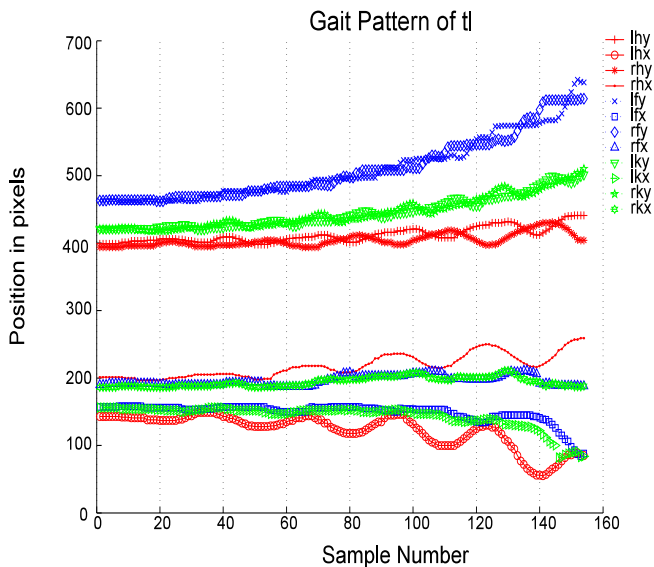
Gait Pattern of tl

Figure 4. Plots of the markers for an unnormalized FN walk

Normalized Gait Pattern of tl
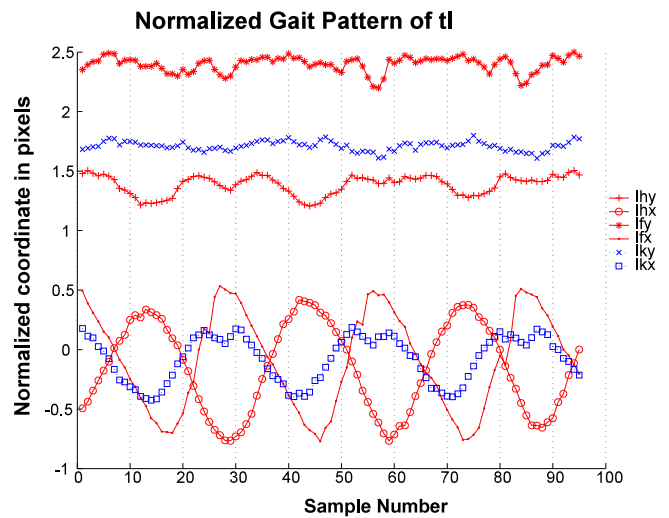
Figure 5. Plot of normalized FP walk

A. Linearity tests

Gait Pattern of cck
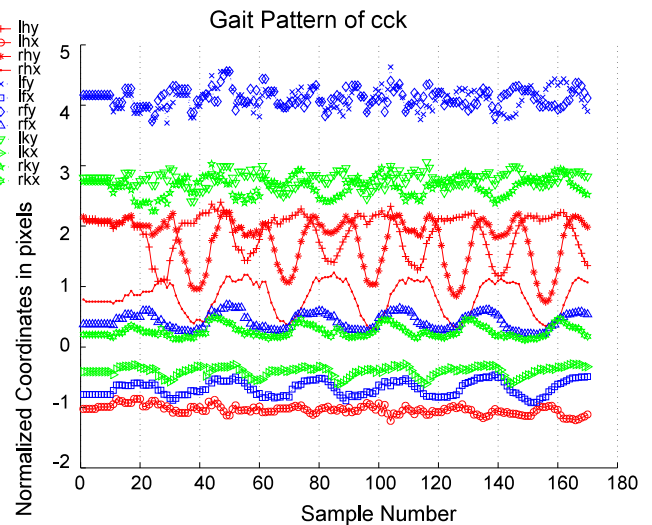
Figure 6. Plots of the markers for a normalized FN walk

In this section we show the results of the tests for signal linearity. The first is the autocorrelation plot for FP gait in Figure 9 which shows strong periodicity in movement, especially in the x-axis which due to its large amplitude swamps out - that is obscures - the "non-periodic" signal in the y-axis when considering the *total* movement of the hand. In contrast, the autocorrelation plot for the FN gait in Figure 7 does not show any periodicity in *any* of the twelve marker trajectories. This is an indicator of nonlinear dynamics or chaotic behaviour. However, it is interesting to note that the motion of a FN walk *silhouette* is periodic [32].

We now look at the results for nonparametric testing of nonlinear behaviour as discussed in Section III.A. The nonlinear prediction error is a discriminating statistic which gives a good test of linearity.

Figure 7. Autocorrelation plot - FN walk of 12 markers

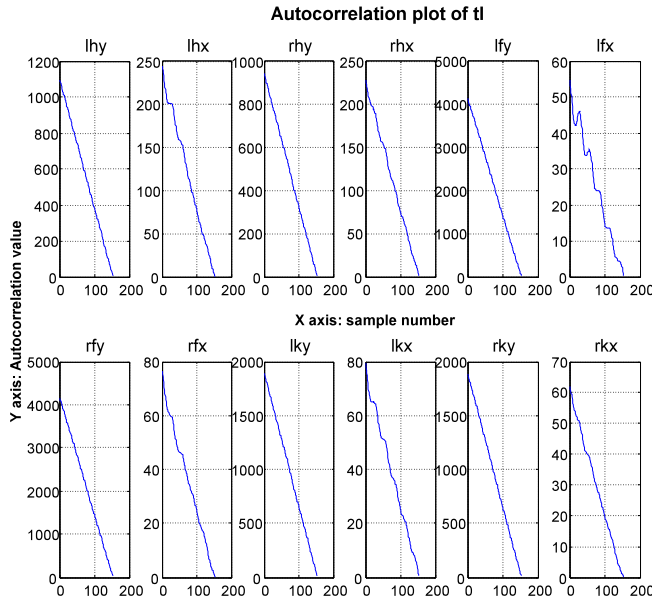It is generated from surrogate data and compared with that from the experimental data. An embedding dimension $m = 2$ was used, with a time delay $\tau = 5$. These values are determined experimentally in Section IV.B. A total of 19 surrogate data series were computed from the movement of one body part. For example in Table 1, *lhy* denotes the values of the movement of the left knee, y axis.
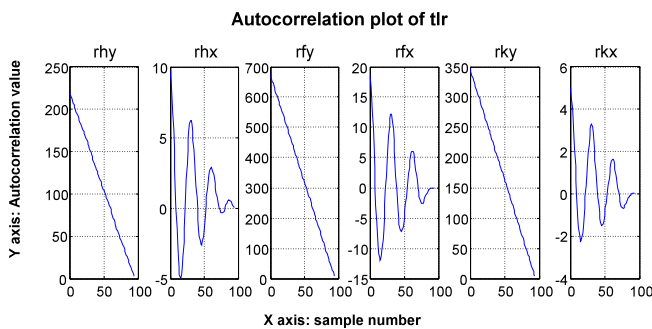

Figure 9. Autocorrelation plot of 6 body markers for FP walk

Here, sMean, sSTD are the mean and standard deviation of the values in all the 19 surrogate data series, *dMean* is the value for the actual data. We use the t-test to see if *dMean* lies within the variability of surrogate data described by *sMean* and

sSTD. The probability column indicates the probability that *dMean* can be described by the null hypothesis H_0 being true. We see that for the first entry the data probably fits H_0, and more weakly for the third entry, but the rest reject H_0. Thus the null hypothesis can be rejected and the data can be considered nonlinear. In Figure 8 we show the plot of the *lhx* marker of a subject and two of its surrogates.
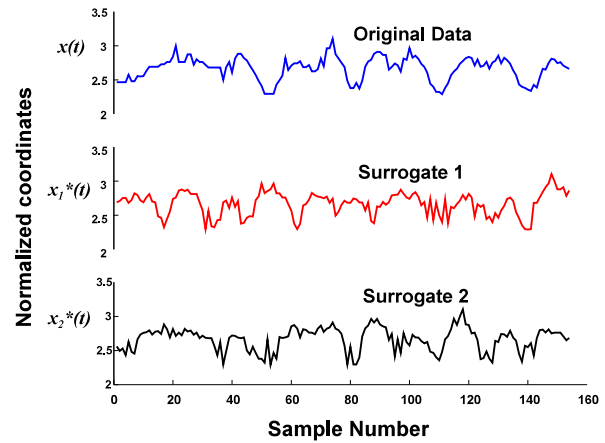
Figure 8. Segmenting the original data and two surrogates for computing statistics

TABLE 1
NONLINEAR PREDICTION ERROR FOR A TYPICAL FN WALK
T-TEST RESULT

	sMean	dMean	sSTD	probability	H_0
lhx	0.176	0.174	0.009	0.814	accept
lhy	0.182	0.119	0.016	0.00	reject
rhx	0.162	0.159	0.009	0.07	accept
rhy	0.145	0.122	0.008	0.00	reject
lfx	0.259	0.227	0.014	0.00	reject
lfy	0.134	0.090	0.011	0.00	reject
rfx	0.231	0.221	0.010	0.00	reject
rfy	0.146	0.109	0.008	0.00	reject
lkx	0.166	0.152	0.009	0.00	reject
lky	0.123	0.104	0.011	0.00	reject
rkx	0.172	0.158	0.010	0.00	reject
rky	0.118	0.090	0.009	0.00	reject

In Table 2, for the FP walk, we include the t-statistic instead of the standard deviation. This is because we see the *x-axis* values, those marked with an '*' in the last column, having high t-statistic values (indicating rejection of H_0) even though they seem strongly periodic. This phenomenon has been described by Stam et al. [33], and is actually an indication of the strongly periodic signals and thus an acceptance of H_0.

TABLE 2
NONLINEAR PREDICTION ERROR FOR FP WALK
T-TEST RESULT
* denotes special non rejection of H_0

	sMean	dMean	t-statistic	Probability	H_0
lhy	0.063	0.045	22.24	0.00	reject
lhx	0.184	0.047	19.97	0.00	accept*
lky	0.064	0.064	1.80	0.64	accept
lkx	0.268	0.037	29.91	0.00	accept*
lfy	0.059	0.064	-6.01	0.00	reject
lfx	0.158	0.087	12.84	0.00	accept*

Since we have evidence of the nonlinearity of FN gait, we have justification for using nonlinear measures on the data from FN gait.

B. Measures of chaosity

Recall in Section III.B, that in order to characterize chaos, a first step is to embed the data into vectors, which require the parameters m and τ, For τ and using the mutual information measure, we show a sample plot in Figure 10 for one person. The point at which the first minimum of the plot is taken to be the best value for τ which is 2 in this case, for all twelve marker trajectories. For m, we use the method of false nearest neighbours (FNN) as described in Section III.B. A typical plot is shown in Figure11. Taking the average of *all* the largest values where the FNN goes to zero, we find the nearest integer value to be six.
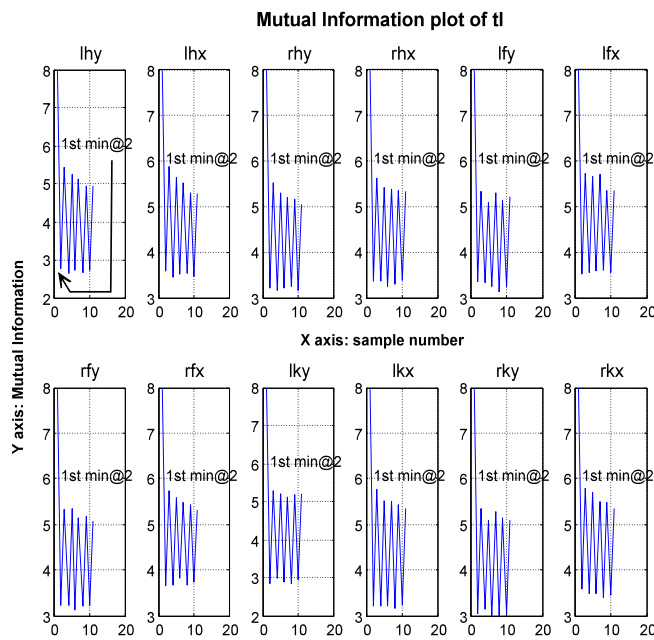

Figure 10. Mutual Information plots - markers of one person in FN walk. Position of first minimum shown in top left subplot.
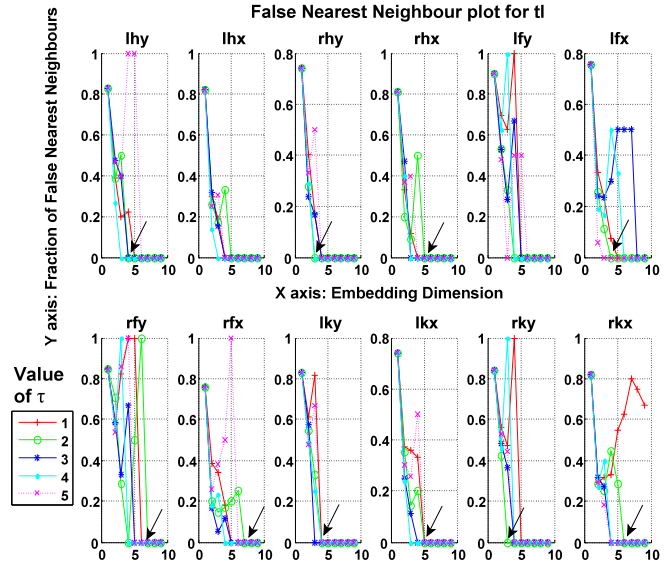

Figure 11. False Nearest Neighbour (FNN) plots for the markers of one person in a FN walk. Arrow marks point where fraction of FNN goes to zero for $\tau = 2$.

V. RESULTS

In this section, we present the results of our experiments on characterizing gait using nonlinear measures of determinstic chaos and also quantities derived from the HHT.

A. Characterizing gait using measures of deterministic chaos

As we have also discussed in Section III.B, the slope of the line fitted to the trajectory will be λ_1. In Figure 12 we see a plot of λ_1 for the twelve marker trajectories of a person. We see that the data is mildly chaotic as λ_1 is positive. As a data reduction measure, we compute the average $\overline{\lambda}_1$ of all the λ_1 of the markers for a subject. An interesting observation in Table 3 is that subjects having similar $\overline{\lambda}_1$ are *s02*, *s03* and s10. We now employ a similar approach for the HHT.

TABLE 3 Values of λ_1 for 12 markers of 3 subjects for τ =2 and m = 5

τ2m5	s02	s02a	s03	s03a	s10	s10a
lhx	1.801	3.710	1.781	2.073	2.242	2.026
lhy	3.726	4.853	2.506	3.572	2.614	1.770
rhx	3.629	2.633	4.016	3.811	2.975	2.582
rhy	3.869	3.333	4.431	3.027	2.962	2.230
lfx	2.495	2.332	2.347	2.112	1.535	1.760
lfy	2.745	1.740	2.256	2.864	2.233	2.219
rfx	2.280	3.145	2.391	2.185	1.985	2.024
rfy	2.832	3.352	3.680	4.267	1.103	3.181
lkx	2.710	2.490	1.988	1.882	2.308	1.644
lxy	4.088	2.641	1.888	2.472	1.912	2.450
rkx	3.395	3.361	2.505	2.173	1.561	1.293
rky	2.877	3.361	3.168	2.538	1.605	2.453
avg	3.037	3.079	2.746	2.748	2.086	2.136
var	0.67	0.76	0.84	0.74	0.56	0.48

tl Lyap exp tau/dim 2/5
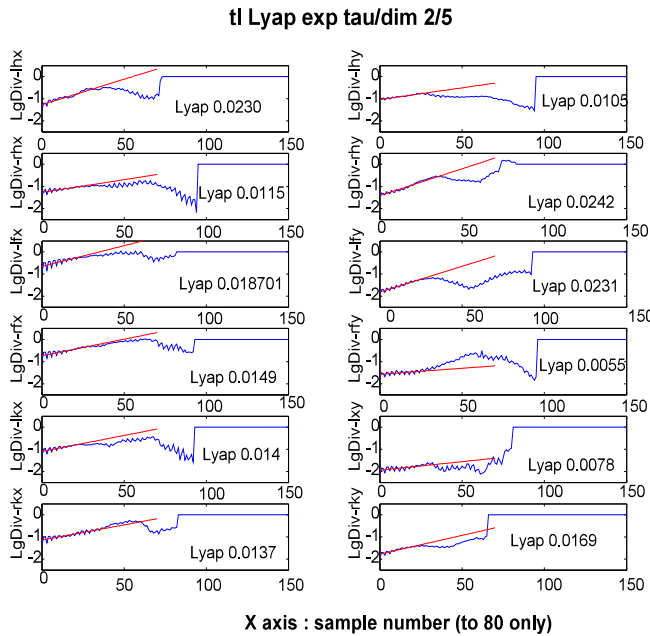

X axis : sample number (to 80 only)

Figure 12. Computation of λ_1 of trajectories of a person's markers using Rosenstein's method as in (2). The y-axis are the log of the divergence and x-axis are the sample numbers. The slope of the average line gives λ_1.

B. Characterizing gait with HHT

The decomposition of the waveform of the *lhx* movement of a subject in Figure 8 (marked "original data") using EMD is shown in Figure 13. Here we show the plots for the IMF and *WMIF*. As we see from the top of the left column of Figure 13 the first few IMF's have a lot of high frequency content accounting for the fine movements of the marker. The frequency decreases with increasing IMFs. While the similarity to frequency decomposition methods like Fourier and wavelet analysis is there, note that the IMF waveforms do not have analytical expressions, hence the empirical nature of EMD. In the right column we see the normalized instantaneous frequency and amplitude at each sample point.

Through experimentation, we found that the third IMF gave the best results, leaving out the knee markers *lkx/y*, *rkx/y* and using *WMIF* instead of the *MIF*. In Table 4, we show the *WMIF* for only the 3 subjects with an extra video sequence. As in the case of chaosity we use as a feature the simple average of all the *WMIF*s of the markers of a subject, excluding the knee markers. This is indicated by the *avg wimf* row at the bottom row of Table 4.

C. Class separability

We apply statistical pattern recognition techniques to our data set even though it is small, to check the feasibility for when a suitable corpus of data is available. We assume that the subjects belong to a class and we examine the separability of the classes and if needed, to see if using other features can help. The values of a feature for a subject are assumed to be normally distributed, the prior probabilities of each class are

the same, and we use the pooled variance as the variance of the data for all the subjects. Since there are only three subjects with a test video, we will use the variance from these groups. The Bhattacharyya distance B_{ij} between classes, defined as:

$$B_{ij}=(1/8)(\mu_i-\mu_j)^T((\Sigma_i+\Sigma_j)/2)^{-1}(\mu_i-\mu_j)$$
$$+(1/2)\ \ln(|(\Sigma_i+\Sigma_j)/2|/(|\Sigma_i|^{1/2}|\Sigma_j|^{1/2})) \tag{6}$$

where μ and Σ are the mean and variance of the classes is used extensively used for measurements of class separability.

TABLE 4 Weighted mean instantaneous frequency for IMF_3 of markers of 3 subjects

marker/subj	s02	s02a	s03	s03a	s10	s10a
lhx	4.16	3.42	3.36	3.5	5.45	3.44
lhy	3.32	4.06	3.52	3.5	2.78	2.55
rhx	3.56	3.91	3.19	3.45	3.26	5.33
rhy	3.86	4.05	4.00	3.35	3.39	3.79
lfx	5.72	4.94	3.78	4.07	6.95	5.19
lfy	3.62	3.21	2.98	1.72	3.2	3.46
rfx	3.19	5.36	3.97	4.48	4.08	6.42
rfy	3.36	3.11	3.36	3.04	3.32	2.26
avg wmif	3.85	4.01	3.52	3.39	4.05	4.06

Since we are using the pooled variance, the log term will be zero. This is more useful than showing the values of $\overline{\lambda}_1$ for *all* the subjects. The results of the calculation between pairs of classes are shown in Table 5 for the $\overline{\lambda}_1$ measure. This is reproduced from [6] for comparison and a more complete discussion. Since the table has are *symmetric* data, in the interests of clarity, we show only the upper diagonal values. We see that some classes are poorly separated with a B_{ij} value (rounded) that is less than or equal to 1. For example classes *s04*, *s06* and *s07* cannot be disambiguated, between *s08* and *s12*, *s02* and *s11* as well.

Similarly, in Table 6 for the *WIMF* classes that cannot be disambiguated are *s01*, *s02*, *s06*, *s08*, *s11* between *s10* and *s11*, and *s05* and *s12*. Making the assumption that the poorly separated classes are not separable, we fuse the $\overline{\lambda}_1$ measure mentioned earlier, so we can successfully classify members of our data set. Now we combine both features to see if we can achieve a better result. We combine both features using a logical AND. For example, if the *avg WMIF* (HHT-based feature) denotes the person being in the group *s01, s02, s06, s08, s11* and the $\overline{\lambda}_1$ (Largest Lyapunov Exponent based feature) being in the group *s04, s06* and *s07*, the person would be *s06*. To save space, we now show the *combined* confusion matrix in Table 7.
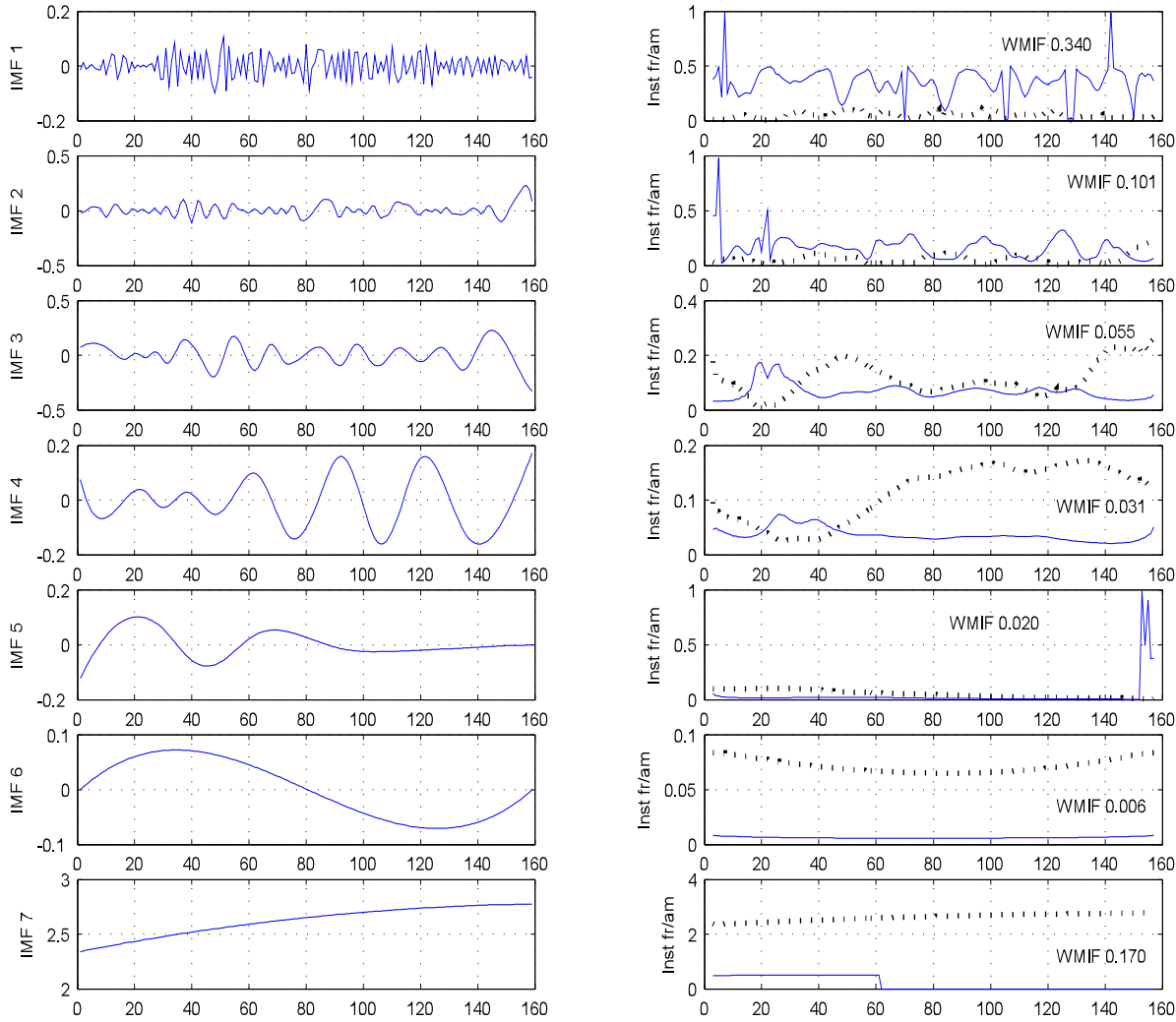
Figure 13. Plots of the (left) first seven IMFs of the *lhx* movement of a subject. On the right is the normalized Instantaneous Frequency (dotted line) and Instantaneous Amplitude (solid line) for the IMF. The Weighted Average IMF is shown as well. The x-axes all denote the sample number.

TABLE 5 Bhattacharyya distance betwen classes using $\overline{\lambda}_1$

	s01	s02	s03	s04	s05	s06	s07	s08	s09	s10	s11	s12
s01	0	85	11	25	11	22	27	3	31	78	75	5
s02		0	36	201	155	190	206	56	14	324	1	51
s03			0	68	43	62	71	3	6	146	29	2
s04				0	3	1	1	45	111	15	185	51
s05					0	2	4	2	2	2	141	29
s06						0	1	103	18	175	2	45
s07							0	48	115	14	190	53
s08								0	15	111	48	1
s09									0	206	10	12
s10										0	303	119
s11											0	43
s12												0

TABLE 6 Bhattacharyya distance betwen classes using HHT

	s01	s02	s03	s04	s05	s06	s07	s08	s09	s10	s11	s12
s01	0	0	4	56	24	1	6	0	7	2	0	20
s02	0	0	8	45	18	0	3	1	11	0	0	14
s03	0	0	0	92	50	10	21	3	0	12	6	44
s04	0	0	0	0	6	40	25	60	104	36	50	8
s05	0	0	0	0	0	15	6	28	59	12	21	0
s06	0	0	0	0	0	0	1	2	15	0	0	11
s07	0	0	0	0	0	0	0	7	26	1	4	4
s08	0	0	0	0	0	0	0	0	6	3	0	23
s09	0	0	0	0	0	0	0	0	0	17	9	52
s10	0	0	0	0	0	0	0	0	0	0	1	9
s11	0	0	0	0	0	0	0	0	0	0	0	17
s12	0	0	0	0	0	0	0	0	0	0	0	0

TABLE 7 Confusion matrix combining HHT and Largest Lyapunov Exponent as features.

PREDICTED/ACTUAL in %

	s01	s02	s03	s04	s05	s06	s07	s08	s09	s10	s11	s12
s01	100											
s02		100										
s03			100									
s04				100								
s05					100							
s06						100						
s07							100					
s08								100				
s09									100			
s10										100		
s11											100	
s12												100

A useful result is that we are able to separate all classes successfully using these two nonlinear measures.

VI. CONCLUSION AND FUTURE WORK

We have used a camera as a sensor to derive the gait signals of a person in a multimedia video data stream. The objective is to see if the data can be used to identify a person. We have shown by using several types of analyses that signals derived from FN gait is nonlinear in nature. This is in contrast to current approaches which impose linear analyses of gait signals for convenience. This gives us a basis for using nonlinear measures of gait. In our experiments, the simple average of the nonlinear features by themselves are not able to discriminate completely between the classes of subjects. However, by combining them, we get a successful result. The novelty of our approach lies in the evaluation and use of both cyclostationarity and nonlinear measures of the gait signal. While our dataset is small, we note that the number of nonlinear features we can extract from the gait signals is potentially very large. A more exhaustive search for features and combinations of signals may yield useful results in terms of deriving new biometrics or improved recognition rates. So future work will need to test this out for current biometrics in a larger dataset and in a markerless environment. There is also much scope for investigating other types of signal analysis that is not based on linearity and stationarity assumptions. By doing so, we capitalize on the ubiquity of video cameras, from which we are able to obtain sensory data which can be used to augment security networks.

REFERENCES

[1] M. W. Whittle, *Gait Analysis: an Introduction*, 4th ed., Philadelphia: Butterworth-Heinemann, 2007, pg 139.

[2] G. Verhoeven, "Did the digital (r)evolution change the concept of focal length?" *AARGNEWS*, vol. 34, pp. 30-35 March 2007.

[3] T. K. M Lee, M. Belkhatir, P.A. Lee and S. Sanei, "Fronto-normal gait incorporating accurate practical looming compensation," *Proc. 19th Int'l Conf. Pattern Recognition (ICPR 2008)*, 2008.

[4] T. Lee, S. Ranganath and S. Sanei, "Patterns in paces: a survey of current approaches in gait recognition," *Proc. Asian Biometric Workshop (ABW 2003)*, pp 421-425, Singapore, Nov. 2003.

[5] A. Veeraraghavan, A. K. Roy-Chowdhury, and Rama Chellapa, "Matching shape sequences in video with applications in human movement analysis," *IEEE Transactions on PAMI*, vol.27, no.12, pp.1896-1909, Dec 2005.

[6] T. Lee, S. Ranganath, and S. Sanei, "Fusion of chaotic measure into a new hybrid face-gait system for human identification," *Proc. ICPR*, Hong Kong, August, 2006.

[7] T. K. M. Lee, K. F. Loe, P. A. Lee and S. Sanei, "A comparison of the basic temporal features of fronto-normal and fronto-parallel gait," *DSP 2007*, Cardiff, UK, July 1-4, 2007.

[8] T. K. M. Lee, S. Sanei and B. Clarke, "Fusion of nonlinear measures in fronto-normal gait recognition," *International Multi-conference on Computing in the Global Information Technology*, Valencia, Spain, 2010.

[9] T. K. M Lee, M. Belkhatir, P. A. Lee and S. Sanei, "Nonlinear characterisation of fronto-normal gait for biometric use," *Proc. Pacific-Rim Conf. On Multimedia (PCM 2008)*, 2008.

[10] H. Tong, "*Non-linear Time Series*" 1st ed, Oxford Science Publications, 1993.

[11] G. Johansson, "Visual perception of biological motion and a model for its analysis," *Perception & Psychophysics*, vol.14, no.2, pp.201-211, 1973.

[12] J. E. Cutting and L. T. Kozlowski, "Recognizing friends by their walk: Gait perception without familiarity cues," *Bull of the Psychonomic Society*, vol.9, no.5, pp.353-356, 1977.

[13] N. F. Troje, "Decomposing biological motion: A framework for analysis and synthesis of human gait patterns," *Journal of Vision*, vol.2, pp.371-387, 2002.

[14] M.S. Nixon, T. Tan and R. Chellappa , "*Human Identification Based on Gait*", 1st ed, Springer, 2005.

[15] R. K. Ibrahim, E. Ambikairajah, B.G. Celler and N.H. Lovell, "Gait pattern classification using compact features extracted from Intrinsic Mode Functions," *30th Ann. Conf. IEEE Engineering in Medicine and Biology Society*, 2008.

[16] N. Wang, E. Ambikairajah, B. G. Celler and N. H. Lovell, "Accelerometry based classification of gait patterns using Empirical Mode Decomposition," *Proc. 2008 IEEE Int'l Conf. Signals, Acoustics and Speech Processing (ICASSP)*, 2008.

[17] P. Kuchi and S. Sethuraman, "Gait recognition using Empirical Mode Decomposition," *Int'l Conf. Advances In Pattern Recognition*, 2003.

[18] G. R. Bradski, "Computer video face tracking for use in a perceptual user interface," *Intel Technology Journal*, vol.Q2, 1998.

[19] T. K. M. Lee, M. Belkhatir and S. Sanei, "Techniques, issues and perspectives for gait-based recognition" (in review) by Pattern Recognition / Elsevier.

[20] J. Theiler, B. Galdrikian, A. Longtin, S. Eubank and J.D. Farmer, "Using surrogate data to detect nonlinearity in time series," *Proc. Nonlinear Modeling and Forecasting, Santa Fe Institute Studies in the Sciences of Complexity, Vol. XII* , Santa Fe, 1992.

[21] T. Schreiber and A. Schmitz, "Discrimination power of measures for nonlinearity in a time series," *Phys. Rev. E*, vol.55, no.5, pp.5443 - 5447, May 1997.

[22] D. Kaplan, "Nonlinearity and Nonstationarity: The use of surrogate data in interpreting fluctuations in heart rate," *Frontiers of Blood Pressure and Heart Rate Analysis*, M. Di Rienzo, et al., IOS Press, 1997.

[23] J. Theiler and D. Prichard, "Constrained-realization Monte-Carlo method for hypothesis testing," *Physica D*, vol.94, pp.221-235, 1996.

[24] F. Takens, "Detecting strange attractors in turbulence," *Lecture notes in Mathematics*, vol. 898, pp. 361-381, Springer-Verlag, 1981.

[25] A. M. Fraser and H.L. Swinney, "Independent coordinates for strange attractors from mutual information," *Phys. Rev. A*, 33, pp. 1134-1140, 1986.

[26] K. B. Kennel, R. Brown and H. D. I. Abarbanel, "Determining embedding dimension for phase-space reconstruction using a geometrical construction," *Phys. Rev. A*, vol. 45, no. 3403, 1992.

[27] M.T. Rosenstein, J. J. Collins and C. J. De Luca, "A practical method for calculating largest Lyapunov exponents from small data sets," *Physica D*, vol. 65, pp. 117, 1993.

[28] H. Kantz, "A robust method to estimate the maximal Lyapunov exponent of a time series," *Physics. Letters A*, vol. 185, pp. 77, 1994.

[29] N. E. Huang, Z. Shen, S. R. Long, M. C. Wu, H. H. Shih, Q. Zheng, N. Yen, C. C. Tung and H. H. Liu, "The empirical mode decomposition and the Hilbert spectrum for nonlinear and non-stationary time series analysis," *Proc. R. Soc. Lond. A*, 454, pp. 903-995, 1998.

[30] N. E. Huang, Z. Shen, and S. R. Long, "A new view of nonlinear water waves: the Hilbert spectrum" *Ann. Rev. Fluid Mechanics*, pp. 415-457, 1999.

[31] E. Hecht, "Optics" , 4th edition, Addison Wesley, 2001.

[32] L. Wang, T. Tan, H. Ning and W. Hu, "Silhouette analysis-based gait recognition for human identification," *IEEE Transactions on PAMI*, vol. 25, no. 12, pp. 1505-1518, Dec 2003.

[33] C. J. Stam, J. P. M. Pijn and W. S. Pritchard, Reliable detection of nonlinearity in experimental time series with strong periodic components, *Physica D*, vol.112, no.3-4, pp.361-380, February 1998.